JOURNAL OF CATALYSIS **76**, 385–392 (1982)

Deactivation Characteristics of an Acrolein Oxidation Catalyst

I. Kinetics of Activity Loss

LEON B. LEVY AND PETER B. DEGROOT

Celanese Chemical Company Technical Center, P.O. Box 9077, Corpus Christi, Texas 78408

Received October 23, 1981; revised March 5, 1982

The thermally induced deactivation of a Mo–V–W–Mn oxide acrolein oxidation catalyst was carried out under air–nitrogen–water vapor atmospheres at 410°C. Catalyst activities were determined in separate experiments using acrolein-containing feed. The rate of deactivation was found to exhibit second-order dependence on catalyst activity. The presence of oxygen is necessary for deactivation to take place, and water vapor, even in very low concentrations, markedly accelerates the deactivation. The deactivation at 410°C can be described by a rate law of the Langmuir–Hinshelwood form:

$$-\frac{d\rho}{dt} = \left[\frac{K_o p_o}{1 + K_o p_o}\right]\left[k_o + \frac{K_w k_w p_w}{1 + K_w p_w}\right]\rho^2$$

where ρ is the relative catalyst activity, K_o and K_w are the adsorption equilibrium constants for oxygen and water, respectively, and k_o and k_w are specific rate constants for the reaction in the absence and in the presence of water, respectively. Estimated values for these constants at 410°C are $K_o = 37\ \text{atm}^{-1}$, $K_w = 250\ \text{atm}^{-1}$, $k_o = 0.13\ \text{hr}^{-1}$, and $k_w = 0.50\ \text{hr}^{-1}$. We conclude that the active site for acrolein oxidation on this catalyst includes an oxygen vacancy. The observed deactivation results from the filling of these vacancies, a process which is facilitated by the presence of surface hydroxyl groups.

INTRODUCTION

The development of bismuth molybdate catalyst by SOHIO in 1956 (*1*) has led to the evolution of commercial processes to selectively oxidize propylene to acrolein, and ultimately acrolein to acrylic acid. A good deal of work has been carried out to elucidate the mechanism of selective olefin oxidation over bismuth molybdate catalysts (*2–6*), and to characterize their structure (*7–10*). Acrolein oxidation catalysts, however, have received relatively little attention in the literature, although many patents have issued on the subject.

Most of the work published to date on the kinetics of catalyst deactivation involves studies of supported noble metal sintering (*11, 12*), and poisoning and coking (*13*). Little information has been forthcoming on the deactivation of selective oxidation catalysts of the mixed metal oxide type. The study described here addresses the factors which influence the rate of deactivation of an acrolein oxidation catalyst. Catalyst deactivation was effected by thermal treatment in air–nitrogen–water vapor atmospheres, and catalyst activity was measured separately with acrolein-containing feed under standard conditions. The information obtained affords some insight into the nature of the active sites on the catalyst.

METHODS

Catalyst preparation. The catalyst studied has the empirical composition $Mo_{12}V_3W_{1.2}Mn_3O_{53}$. It was prepared according to the method specified by Allen (*14*) as follows. To a stirred solution of ammonium heptamolybdate tetrahydrate (42.4 g in 100 ml of water) at 60°C was slowly added ammonium metavanadate (7.0 g in 100 ml of water), ammonium paratungstate hexahy-

0021-9517/82/080385-08$02.00/0

drate (6.1 g in 100 ml of water), and manganese acetate tetrahydrate (15.0 g in 50 ml of water). The suspension was evaporated to dryness under a stream of air by rotating the flask in a 120°C oil bath. The resulting solid was calcined at 385°C in an air atmosphere for 5 hr and ground to a particle size of −20 + 30 mesh (0.59 to 0.84 mm).

Deactivation treatment. The reactor used for the deactivation treatment was a 316 stainless-steel U tube having an internal diameter of 9.25 mm. A charge of 15.0 g of the catalyst was placed in the reactor, and the reactor inlet connected to a source of the desired gas. A gas flow of 200 cm^3/min was then started, and the reactor was immersed in an air-fluidized sandbath thermostated at the desired temperature. After a chosen time interval the reactor was purged with nitrogen, removed from the sandbath, and cooled with the nitrogen still flowing. The catalyst was discharged, and a 1.0 g sample taken for activity measurement (see below). The remainder of the catalyst was recharged to the reactor, and the treatment continued.

Predrying procedure. The following catalyst pretreatment drying procedure was added to the deactivation treatment after it was found that the rate of deactivation was very sensitive to the catalyst's hydration state. After the catalyst was charged to the reactor (see above) a flow of 200 cm^3/min of P_2O_5-dried nitrogen was passed through the reactor for 10 min at room temperature, and then for 16 hr at 200°C. With the nitrogen still flowing the reactor was removed from the sandbath and cooled to room temperature. At this point the flow of nitrogen was stopped, and that of the gas to be used in the deactivation treatment was started (without opening the reactor). The air and nitrogen used were dried by passing through a bed of fresh P_2O_5. The reactor was placed in a sandbath thermostated to the deactivation treatment temperature, and the kinetic run started.

The catalyst was also treated for 1 hr at 200°C in dry nitrogen after each time the reactor was opened to remove a kinetic sample.

Determination of catalyst activity. The catalyst activity measurements were made on a 1.0 g sample of catalyst diluted with 16.1 g of Norton Crystolon grade 24× grit silicon carbide. The diluted material was charged to the same type of reactor used in the deactivation treatment (see above) and fed with 630 cm^3/min (1 atm, 25°C) of a gas stream containing 4 mol% acrolein, 5 mol% O_2, 48 mol% N_2, and 43 mol% water vapor. The reactor was immersed in a sandbath thermostated to 285°C, and the system pressure controlled at 2.7 atm. The acrolein conversion was determined by gas chromatographic analysis of the product stream. These conditions simulate realistic operation of the catalyst, and do not result in any catalyst deactivation during the test period.

A reliable mathematical model for this fixed bed catalytic reaction had been developed based on a two-dimensional, multicell technique proposed by Kuester (*15*). The use of this model enabled us to calculate accurately the relative catalyst activity from the acrolein conversion in a microreactor in which the conditions (specified above) were not gradientless.

A key characteristic of the catalyst deactivation being studied is the fact that the selectivities to various products remain constant as the activity declines. This implies that the deactivation is a result of a

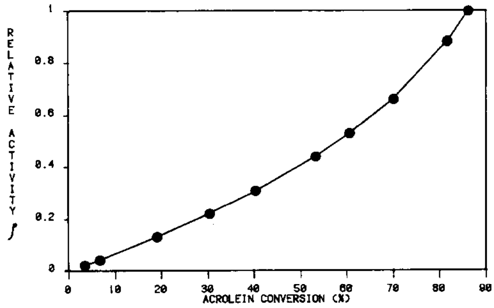

FIG. 1. Relative catalyst activity (ρ) from acrolein conversion in the microunit test at 285°C.

homogeneous decrease in the density of all sites, rather than selective site disappearance or a change in the nature of the sites. Therefore, for the kinetics included in the mathematical model for acrolein oxidation we defined a relative site density coefficient, ρ, which was prefixed to the Arrhenius expression defining each rate constant in the reaction network, such that $k_i = \rho A_i \exp(-E_i/RT)$. k_i, A_i, and E_i are the rate constant, Arrhenius preexponential, and activation energy for the ith step in the reaction network. We shall henceforth refer to the relative site density coefficient, ρ, as the relative catalyst activity.

The relationship between acrolein conversion in our microunit activity test and the relative catalyst activity, ρ, is illustrated in Fig. 1. In all our deactivation experiments we characterized the kinetics of deactivation by determining the values of ρ in samples taken from the deactivation treatment (see above) at increasing time. Interestingly, none of the general conclusions reached in this work would have been qualitatively different had we used acrolein conversion itself as the key measure of catalyst activity.

RESULTS AND DISCUSSION

General Effects of Gas Composition

At the outset of our work, we sought to determine whether the catalyst deactivated via simple thermal sintering, poisoning, coking, or some other mechanism. From previous experience it was known that the rate of deactivation at 410°C would be easily measurable over convenient time periods. To follow the deactivation under actual acrolein oxidation conditions at this high a temperature we operated the catalyst as described in the section entitled "Determination of Catalyst Activity," except that the bed was composed of 0.15 g of catalyst diluted with 16.1 g silicon carbide. The acrolein conversion declined from an initial value of 61 to 43% over a 48-hr period. For these reaction conditions this represented a drop in relative activity (ρ) from unity to 0.58. This was the only experiment where the catalyst was deactivated under actual reaction conditions. In all other cases the deactivation was carried out under air-nitrogen–water vapor atmospheres.

In a control run a sample of the catalyst was heated to 410°C under a stagnant air atmosphere for 48 hr. Live feed was introduced only initially (and then flushed out with air) and terminally to determine the decrease in activity. By the end of the run the value of ρ had dropped to 0.43. This represented more extensive deactivation than we had measured in the run with acrolein feed. This indicated that the rate of deactivation might be a positive function of the oxygen partial pressure. To confirm this dependence we carried out an experiment in which the catalyst was treated with a 20 cm^3/min air flow at 410°C for 16 hr. The final value of ρ was 0.15.

This run was repeated seven times, substituting pure nitrogen for the air atmosphere. Even though, in some cases, the treatment time was extended to 67 hr, in no case was any deactivation detectable. In fact, a 5-hr treatment of the catalyst under nitrogen *at 450°C* only resulted in a drop in the value of ρ to 0.8.

It was also observed in catalyst thermal treatments at 370°C that the rate of deactivation increased by a factor of about 2 when the atmosphere was changed from 100% air to 50 mol% air, 50 mol% water vapor.

Changes in Physical Properties during Deactivation

We determined using X-ray fluorescence analysis that there was no measurable loss of molybdenum from the catalyst during deactivation treatments (the precision of the analyses was ±1% of the amount present). We had previously determined in separate experiments that molybdenum deficiencies of up to 5% do not affect catalyst activity.

No change in weight could be detected using thermogravimetric analysis (TGA) when the catalyst was heated in air at 410°C (the detectable limit is 0.3%).

In a number of the early deactivation runs with air we measured the specific surface area for each kinetic sample tested for activity. In general, the relative activity (ρ) fell much more rapidly than the relative surface area. At the end of one run, for instance, half the surface area remained, while the catalyst retained only 10% of its initial activity.

This disparity in the rates of loss of activity and of surface area led us to conclude that the deactivation is not a simple function of gross sintering. Either it does not involve sintering at all (i.e., the surface area is being lost from a catalytically inactive phase), or the surface area of the active phase is only a small part of the total surface area, and it diminishes at a relatively rapid rate compared to the total sintering rate.

A confirmation of the deep-seated changes occurring in the catalyst during deactivation was forthcoming from a study of X-ray diffraction pattern changes which take place concurrently. This study is described in detail in the following paper (*16*). It will suffice to mention here that as the catalyst is deactivated in air there is a transition from an essentially amorphous structure to one with a well-resolved diffraction pattern rich in peaks. The position of these peaks depends on the composition of the atmosphere during treatment; the areas of selected peaks correlate well with the extent of deactivation.

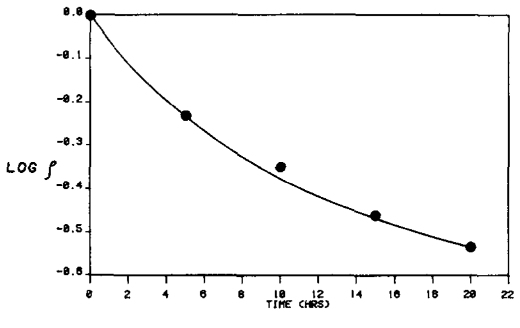

FIG. 2. Catalyst deactivation in air at 410°C (first-order plot).

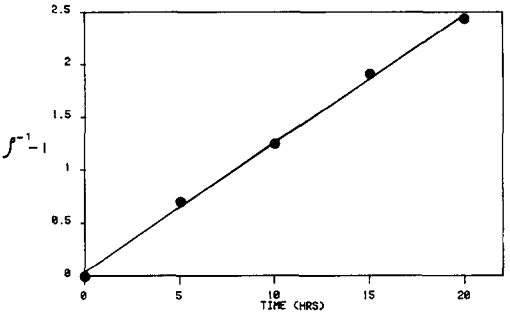

FIG. 3. Catalyst deactivation in air at 410°C (second-order plot).

Deactivation Rate: Kinetic Order in Oxygen and in Catalyst Activity

The preliminary experiments described above gave us some indications of the order of magnitude of the deactivation rate at 410°C, and the effect of gas composition. In order to determine more accurately the deactivation rate in air at 410°C, we carried out multipoint experiments lasting about 30 hr in which five or six samples were taken for activity measurement during the deactivation. The activity–time plots were linear when plotted as second order in ρ (see below). We noted, however, that the apparent rate constants were not reproducible, varying from about 0.1 to 0.3 hr^{-1}. This irreproducibility was ultimately attributed to traces of moisture (10 to 20 ppm) in the industrial cylinder air supply used in the deactivation treatments. Using "zero" grade air, or passing the air through a zeolite drying tube did not solve the problem. Only when the air was dried with P_2O_5 did the results become reproducible.

Figures 2 and 3 show, respectively, the actual data points of a P_2O_5-dried air run plotted as first- and second-order processes with respect to the relative activity, ρ. It is evident that the second-order plot is more linear. This observation holds true for all of the kinetic deactivation runs carried out.

By using various air–nitrogen blends at

410°C we carried out deactivation runs at oxygen partial pressures (p_0) of 0.210, 0.158, 0.105, 0.0840, 0.0525, and 0.0210 atm. We calculated an apparent deactivation rate constant, k_a, for each run from the slope of the least-squares line for a plot of $\rho^{-1} - 1$ versus treatment time. The results are presented in Table 1. There is a definite correlation between the apparent rate constant, k_a, and oxygen partial pressure. A plot of k_a versus p_0 is concave downward. A linear plot of $1/k_a$ versus $1/p_0$ would suggest a p_0 functionality in the rate law formally analogous to Langmuir–Hinshelwood format, e.g.,

$$-\frac{d\rho}{dt} = k_a\rho^2 = \left[\frac{k_0K_0p_0}{1 + K_0p_0}\right]\rho^2. \qquad (1)$$

Such a plot is shown in Fig. 4. Although there is a good deal of scatter to the points, we feel that the correlation coefficient of 0.91 for the least-squares line is high enough to warrant our using Eq. (1) as a reasonably descriptive rate law.

From the slope and intercept of the least-squares line in Fig. 4 we estimate that at 410°C the values of K_0 and k_0 are 37 atm^{-1} and 0.13 hr^{-1}, respectively.

Deactivation Rate: Kinetic Order in Water Vapor

As mentioned above, parts per million concentrations of moisture in the air supply during deactivation caused significant fluctuations in the deactivation rate. Moreover, the rate responded to differences between the moisture content of air dried by passing through a molecular sieve and through P_2O_5. These are surely subtle differences between very low concentrations, and yet these differences were significant enough to affect the rates of deactivation.

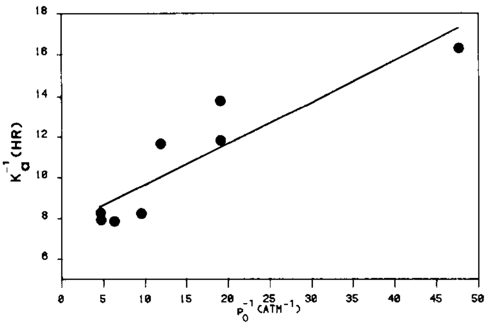

FIG. 4. Effect of oxygen partial pressure (p_0) on the apparent deactivation rate constant (k_a) at 410°C. (Reciprocal–reciprocal plot.)

We systematically varied the water partial pressure in the gas atmosphere in a series of deactivation treatments at 410°C. The second-order rate plots were linear, and gave the apparent rate constants, k_b, shown in Table 2.

To help formulate a suitably descriptive rate law format, we carried out several runs at 410°C in which the gas atmosphere consisted only of nitrogen and water vapor. The rates were immeasurably low. This indicates that the deactivation rate law has

TABLE 1

Effect of Oxygen Partial Pressure (p_0) on the Apparent Deactivation Rate Constant (k_a) at 410°C

p_0 (atm)	k_a (hr^{-1})
0.2100	0.126, 0.122
0.1575	0.127
0.1050	0.121
0.0840	0.0856
0.0525	0.0724, 0.0844
0.0210	0.0613

TABLE 2

Effect of Water Vapor Partial Pressure (p_w) on the Apparent Deactivation Rate Constant (k_b) at 410°C

p_w (atm)	p_0 (atm)	k_b (hr^{-1})	ψ (hr^{-1})[a]
0.255	0.157	0.583, 0.697	0.551, 0.685
0.102	0.189	0.699	0.667
0.051	0.199	0.354	0.271
0.013	0.207	0.481	0.412
0.0010	0.209	0.207	0.102

[a] $\psi = [(1 + 37.4\,p_0)\,k_b]/37.4\,p_0 - 0.131$ (see text for significance of this parameter).

two terms, each of which degenerates to zero in the absence of oxygen, e.g.,

$$-\frac{d\rho}{dt} = k_b\rho^2 = \left[\frac{K_o p_o}{1 + K_o p_o}\right]\left[k_o + \frac{K_w k_w p_w}{1 + K_w p_w}\right]\rho^2. \quad (2)$$

The integrated form of this equation is

$$\rho^{-1} - 1 = \left[\frac{K_o p_o}{1 + K_o p_o}\right]\left[k_o + \frac{K_w k_w p_w}{1 + K_w p_w}\right] t. \quad (3)$$

Rearranging, and substituting the estimated values of k_o and K_o found for Eq. (1) at 410°C, we get

$$\frac{K_w k_w p_w}{1 + K_w p_w} = \frac{(1 + 37.4\, p_o)k_b}{37.4\, p_o} - 0.131 \equiv \psi. \quad (4)$$

The value of ψ, the contribution of water vapor to the deactivation rate, was evaluated for each experiment with water vapor present, and the calculated values included in Table 2. If Eq. (2) is reasonably descriptive of the kinetics, a plot of $1/\psi$ versus $1/p_w$ should be linear. Such a plot is shown in Fig. 5. Although there is again quite a bit of scatter, we can estimate that at 410°C the values of K_w and k_w are 250 atm^{-1} and 0.50 hr^{-1}, respectively.

Mechanism of Deactivation

The present study represents a first step in the characterization of a previously neglected process. The results enable us to draw some general conclusions regarding the nature of the active sites, and the type of process involved in their disappearance.

First of all, since oxygen is indispensable to the deactivation process at these temperatures, we must conclude that the active sites involve lattice oxygen vacancies or metal atoms in lower than maximum valence states. The deactivation process thus appears to be an oxidation. The density of oxygen vacancies must be quite low, since no weight increase can be detected by TGA on heating the catalyst in air at 410°C. These conclusions are analogous to those of Nováková *et al.* who observed that partially reduced bismuth molybdate was more active in oxidizing propylene or acrolein than the fully oxidized material (*17*).

We have observed that the deactivation rate can be influenced profoundly by extraordinarily low concentrations of water vapor in the atmosphere. This leads us to propose that the presence of very low surface concentrations of strongly adsorbed water (perhaps fractions of a monolayer) is quite potent in facilitating the oxidation of the lattice vacancies associated with active sites. It is also possible that the second order of the kinetics with respect to activity reflects involvement of a pair of oxygen vacancies from nearby active sites with a single oxygen molecule. One could also visualize the presence of surface hydroxyl groups (arising from water adsorption) leading to a lower energy path for oxidizing the vacancies. Possible mechanisms are shown below.

"Dry" Reaction

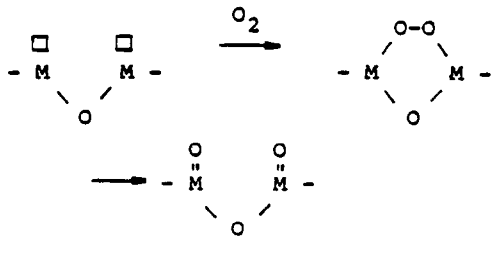

"Wet" Reaction

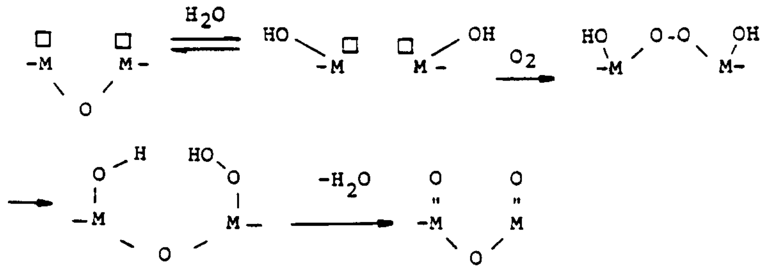

These are simply examples of the many vacancy oxidation mechanisms which can be written for both "dry" and "wet" catalyst surfaces. The viability of these mechanisms does not depend upon the particular form of oxygen or water vapor functionality chosen for the rate law.

The observation that adsorbed water labilizes surface redox reactions has some precedence. Previous workers have noted that water is necessary for the oxidation of acrolein over mixed oxide molybdenum catalysts, and that if $H_2{}^{18}O$ is used ^{18}O is incorporated into the acrylic acid product (*18*, *19*).

Sotani (*20*) noted that when partially reduced molybdenum trioxide was exposed to water vapor (no oxygen present) at 400°C the Mo^{V} ESR signal intensity diminished very rapidly. He attributed this effect to the destabilization of Mo^{V} by adsorbed water, and its disproportionation to other valence states, e.g., Mo^{IV} and Mo^{VI}. In the system studied here, water accelerates the deactivation, but the presence of oxygen is necessary for it to occur at all. It would seem, therefore, that the deactivation in our case involves actual incorporation of gas phase oxygen into the lattice structure.

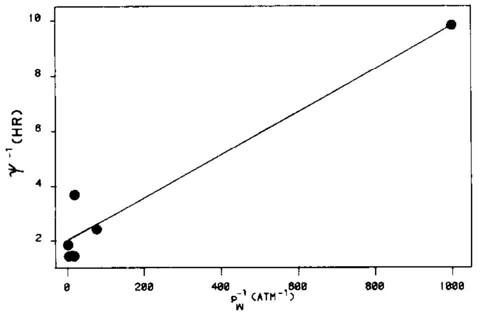

FIG. 5. Contribution (ψ) of water partial pressure (p_w) to the deactivation rate at 410°C. (Reciprocal-reciprocal plot.)

It is certainly not unreasonable to picture a surface oxygen vacancy as part of an active site for acrolein oxidation. Such a vacancy would be a likely site for chemisorption of acrolein through metal to carbonyl oxygen complex formation. The actual abstraction of lattice oxygen, however, would most likely be from a neighboring, fully oxidized metal atom.

Finally, it should be noted that there is certainly a large body of evidence indicating that oxides of molybdenum, tungsten, and vanadium can contain oxygen vacancy defects. These range from random, isolated vacancies, to short- and even long-range ordered defect structures (*21–23*). Our postulation that such vacancies comprise part of the surface active sites in acrolein oxidation is made more credible considering the facility with which these defects are thought to move through the crystal structure (*24*).

ACKNOWLEDGMENTS

The authors wish to thank C. A. Dalton, Y. Urban, H. Ramos, and P. Hernandez for their help in carrying out the experimental work.

REFERENCES

1. Callahan, J. L., Foreman, R. W., and Veatch, F., U.S. Patent 2,941,007 (assigned to Standard Oil Co., Ohio), June 14, 1960.

2. Adams, C. R., and Jennings, T. J., *J. Catal.* **2,** 63 (1963).
3. Wragg, R. D., Ashmore, P. G., and Hockey, J. A., *J. Catal.* **22,** 49 (1971).
4. Matsuura, I., and Schuit, G. C. A., *J. Catal.* **20,** 19 (1971).
5. Krenzke, L. D., Keulks, G. W., Sklyarov, A. V., Firsova, A. A., Kutirev, M. Yu., Margolis, L. Ya., and Krylov, O. V., *J. Catal.* **52,** 418 (1978).
6. Otsubo, T., Miura, H., Morikawa, Y., and Shirasaki, T., *J. Catal.* **36,** 240 (1975).
7. Keulks, G. W., *J. Catal.* **19,** 232 (1970).
8. Sleight, A. W., Linn, W. J., and Aykan, K., *Chemtech* **8,** 235 (1978).
9. Matsuura, I., and Schuit, G. C. A., *J. Catal.* **25,** 314 (1972).
10. Kumar, J., and Ruckenstein, E., *J. Catal.* **45,** 198 (1976).
11. Herrmann, R. A., Adler, S. F., Goldstein, M. S., and DeBaun, R. M., *J. Phys. Chem.* **65,** 2189 (1961).
12. Maat, H. J., and Moscou, L., *in* "Proc. Third Int. Cong. on Catal." (W. M. H. Sachtler, G. C. A. Schuit, and P. Zwietering, Eds.), Vol. II, p. 1277. North-Holland Publishing, Amsterdam, 1965.
13. Butt, J. B., *AIChE J.* **22,** 1 (1976).
14. Allen, G. C., U. S. Patent 3,644,509 (assigned to Celanese Corp.), February 22, 1972.
15. Kuester, J. L., "Two Dimensional Model Simulation of Fixed Bed Catalytic Reactors." Ph.D. Dissertation, Texas A and M University, January, 1970.
16. DeGroot, P. B., and Levy, L. B., *J. Catal.* **76,** 393 (1982).
17. Nováková, J., Jírů, P., and Zavadil, V., *Coll. Czech. Chem. Commun.* **37,** 1233 (1972).
18. Nováková, J., Dolejšek, Z., and Habersberger, K., *React. Kinet. Catal. Lett.* **4,** 389 (1976).
19. Zhiznevskii, V. M., and Yakubovskaya, L. F., *Kinet. Katal.* **17,** 953 (1976).
20. Sotani, N., *Rev. Phys. Chem. Japan* **46,** 1 (1976).
21. Kihlborg, L., *in* "Advances in Chemistry Series" (R. Ward, Chairman), Vol. 39, p. 37. American Chemical Society, Washington, D. C., 1963.
22. Bursill, L. A., *Proc. Roy. Soc., Ser. A* **311,** 267 (1969).
23. Wadsley, A. D., *Rev. Pure Appl. Chem. (Aust.)* **5,** 165 (1955).
24. Anderson, J. S., and Hyde, B. G., *Bull. Soc. Chim. France* **1965,** 1215.